

## RESEARCH / INVESTIGACIÓN

# Successful *in-vivo* treatment of mice infected with *Candida glabrata* using silver nanoparticles

Teeba H. Mohammad<sup>1</sup>, Mohsen H. Risan<sup>1</sup>, Gamal A. El-Hiti<sup>2\*</sup>, Dina S. Ahmed<sup>3</sup>, Emad Yousif<sup>4</sup> DOI. 10.21931/RB/2020.05.04.10

**Abstract:** The current study describes the production of silver nanoparticles (AgNPs) to treat *Candida glabrata* infections. The method involved incubation of silver nitrate (AgNO<sub>3</sub>) with *Aspergillus terreus* using a green and straightforward route. The production of AgNPs was confirmed through a color change from transparent yellow to brown as well as by ultraviolet-visible (UV-VIS) spectroscopy. The surface morphology of AgNPs was assessed using a scanning electron microscope. The antifungal activity of AgNPs against *C. glabrata* was investigated in the serum of 20 infected mice. The mice were divided into four groups, and the level of cytokines: IL-4 and IFN- $\gamma$  were examined after 21 days. The atomic force microscopy confirmed that the average diameter of AgNPs was 25.1 nm, which is appropriate for delivering silver nanoparticles to treat animals' infection. The concentration of cytokines IL-4 and IFN- $\gamma$  were significantly ( $P < 0.05$ ) higher in the *C. glabrata*-infected group than in the control group. While the cytokines level remained close to average concentration in mice administrated with AgNPs, such a result was comparable with the fourth group of mice (*Candida*-treated *Aspergillus*) after treatment with AgNPs.

**Key words:** *Candida glabrata*, *Aspergillus terreus*, cytokines, silver nanoparticles, antifungal activity, surface morphology.

## Introduction

*Candida* is a genus of ascomycetes, yeast containing approximately 150 species of which more than 20 have clinical importance<sup>1</sup>. *Candida species* (spp.) cause several fungal infections and are considered the fourth most common cause of bloodstream infections (BSIs) in the general population<sup>2</sup>. Candidemia is expected in the USA, where it poses a severe health risk<sup>3</sup>. However, *Candida albicans* and *Candida glabrata* remain the primary cause of aggressive candidiasis since they contribute to 50% of all cases of infections<sup>4</sup>. The most common risk factors associated with *Candida* BSI are malignancy, disruption of mucosal barriers, sustenance broad-spectrum antibiotics, immune suppression due to radiotherapy or chemotherapy, and urinary catheterization<sup>5</sup>.

Candidemia causes various severe illnesses and is not susceptible to many antifungal agents. Four common types of antifungal drugs, azoles, polyenes, flucytosine, and echinocandins, are effective against candidiasis<sup>6</sup>. Nonetheless, in most cases, the infection poses a mortality risk, and treatment is expensive and therapeutic effectiveness brutal to achieve<sup>7</sup>. Therefore, discovering a novel antifungal treatment is a vital strategy to control the infection and overcome antifungal resistance<sup>8</sup>. In recent years, nanoparticles have received substantial attention as a novel approach in developing useful materials with unique chemical and physical properties<sup>9</sup>. Such materials can be used exclusively in various fields such as medicine, biology, chemistry, health care, food, and industry<sup>10,11</sup>. Several synthetic procedures have been used to produce nanoparticles in which the size and shape of particles can be controlled<sup>12</sup>. These methodologies are sustainable, eco-friendly, and involve the in-vivo use of eukaryotes<sup>13,14</sup>.

Silver nanoparticles (AgNPs) have been widely used in the production of antimicrobial agents, drug delivery, medical devices, household-uses, cosmetics, optical sensors, and pharmaceuticals<sup>15</sup>. Various processes have been developed for the synthesis of AgNPs. However, most synthetic methods are expensive to run and involve the use or production of hazar-

dous materials<sup>16</sup>. Nevertheless, researchers have given much attention and are investigating the biological process as an alternative to synthetic processes in synthesizing AgNPs<sup>16</sup>. Such biological processes are environment-friendly, simple, high-yielding, inexpensive to run, and does not produce or use poisonous chemicals. Besides, AgNPs produced biologically have high stability and solubility, well-defined morphology, and appropriate particle size<sup>16</sup>.

Many plants, fungi, and bacteria have been involved in the biological synthesis of AgNPs. Various fungal species, such as ascomycete and basidiomycete, can stabilize and reducing agents in the biological synthesis of AgNPs, including the intracellular and extracellular formation of *Aspergillus terreus*<sup>17-19</sup>. Mycelium, mycelium broth, and fungi substrate are used mainly in the AgNPs biosynthetic methods<sup>20</sup>. The biosynthesis of AgNPs involves culturing a fungus on agar followed by transfer to a liquid medium to produce biomass. Silver nitrate (AgNO<sub>3</sub>) is then incubated with fungus in a controlled environment to produce AgNPs<sup>21</sup>. Various AgNPs have been synthesized and used as antimicrobial agents. For example, AgNPs synthesized using *A. fumigatus* showed cytotoxic, antibacterial activities<sup>22</sup>. Also, *A. terreus* obtained from *Calotropis procera*, was used to synthesize AgNPs that act as an antibacterial against *Salmonella typhi*, *Staphylococcus aureus*, and *Escherichia coli*<sup>23</sup>. Similarly, *A. terreus* has been used to produce AgNPs with antimicrobial activities against *C. albicans*, *C. krusei*, *A. fumigates*, *A. niger*, *A. ochraceus*, and *S. aruras*<sup>24</sup>. The AgNPs synthesized using *Andrographis paniculata* were used as antimicrobial against *S. typhi* and *S. aureus*<sup>25</sup>.

The effect of a mixture of AgNPs and an antifungal agent such as fluconazole has been investigated against several pathogenic fungi<sup>26</sup>. The development of distinct cytokines in mice is essential in stimulating the practical outcome of host-defense against a fungal infection<sup>27</sup>. Resistance to *Candida* BSI requires the harmonized action of innate and adaptive immunity. *Candida*'s distinct feature is the morphological change to the

<sup>1</sup> Department of Molecular and Medical Biotechnology, College of Biotechnology, Al-Nahrain University, Baghdad, Iraq.

<sup>2</sup> Cornea Research Chair, Department of Optometry, College of Applied Medical Sciences, King Saud University, Riyadh, Saudi Arabia.

<sup>3</sup> Department of Medical Instrumentation Engineering, Al-Mansour University College, Baghdad, Iraq.

<sup>4</sup> Department of Chemistry, College of Science, Al-Nahrain University, Baghdad, Iraq.

Corresponding author: gelhiti@ksu.edu.sa

hyphal form, which is associated with virulence factors. Phagocytosis of the *Candida spp.* induced mice dendritic cells to produce cytokines<sup>28</sup>. Previous work concentrated on the successful *in-vitro* use of AgNPs as antimicrobial agents. Therefore, the current study aims to produce AgNPs using *A. terreus* based on previous reports<sup>18-20</sup> and their use in the treatment of *C. glabrata* in an animal model. *Candida* BSI's effective treatment in infected mice with *C. glabrata* in which the level of cytokines: (interleukin-4) IL-4 and interferon-gamma (IFN- $\gamma$ ) were measured. The current work reported an efficient and successful *in-vivo* treatment of mice infected with *C. glabrata* with AgNPs in which serum cytokines level was monitored.

## Methods

### Preparation of biomass

*A. terreus* was isolated from soil and grew on Czapek Dox Agar for 72 h at 25 °C. The identification of pure isolates was based on color changes and microscopic and morphological observations. Biomass of *A. terreus* was grown aerobically in a liquid medium containing KH<sub>2</sub>PO<sub>4</sub> (47 g), K<sub>2</sub>HPO<sub>4</sub> (2 g), MgSO<sub>4</sub> 7H<sub>2</sub>O (0.1 g), (NH<sub>4</sub>)<sub>2</sub>SO<sub>4</sub> (1 g), yeast extract (0.6 g), and glucose (10 g) in one liter. The culture was kept in a sterile flask (250 mL) and inoculated at 25 °C. In another sterile flask, fresh biomass (20 g) was added to distilled water (200 mL) and kept for 72 h at 25 °C. The mycelia were harvested through filtration using a Whatman filter paper (GE Healthcare Life Science, Chicago, IL, USA) (grade 1). Mycelia were washed with sterilized distilled water to remove any residues from the medium.

### Extracellular synthesis of AgNPs

The *A. terreus* filtrate (20 mL) was treated with AgNO<sub>3</sub> (200 mL; 100 mM), and the flask was incubated in the dark at 25 °C for 24 h. The fungal filtrate color change recognized the production of AgNPs from transparent yellow to brown. The AgNPs were centrifuged (10,000 rpm) for 10 min, and the process was repeated for two times to produce a pellet that dried for use. The AgNPs were collected and characterized. The pure fungal filtrate (without AgNO<sub>3</sub>) was used as a positive control. While pure AgNO<sub>3</sub> (1 mM) was used as a negative control.

### Characterization of AgNPs

The UV-VIS spectrum of AgNPs was recorded on a UV-Vis-NIR-V670 spectrophotometer (JASCO Corp., Tokyo, Japan). The external surface morphology and particle dimensions of the synthesized AgNPs were inspected by the AA3000 SPM system AFM (Shimadzu Co., Kyoto, Japan). Droplets of AgNPs on a glass slide were examined using a NTEGRA SPECTRA II NT-MDT (Spectrum Instruments Ltd., Moscow, Russia) at room temperature. The surface of the synthesized AgNPs was inspected by the TESCAN VEGA3 SEM (TESCAN Analytics, Brno-Kohoutovice, Czech Republic). Species identification and antifungal susceptibility were performed using the API ID 32 C (bioMérieux Corp., Marcy-l'Étoile, France).

### Experimental procedures

The VITEK 2 compact system (BioMérieux Inc., Durham, NC, USA) was used to identify *C. glabrata*. A group of mice consists of 20 healthy males (6-weeks-old) with a weight that ranged from 20 to 25 g. Mice were captured in stainless steel cages at a controlled temperature (22 ± 2 °C) and moisture (55 ± 10%). The mice were provided with nutrients and water

daily for 21 days and divided into four groups ( $n = 5$  in each group). The control group of mice received physiological saline solution (1 mL). The *Candida* (non-treated) group of mice was infected with *C. glabrata* (10<sup>5</sup>, 0.2 mL). The third group of mice was provided with AgNPs synthesized with *A. terreus* only (10  $\mu$ g). The fourth group (treated) of mice was infected with *C. glabrata* a week after AgNPs had treated them synthesized with *A. terreus* (10 mg), as a suspension. After 21 days of treatment, mice were killed using ketamine-xylazine anesthesia for 1–2 h. The anesthesia consists of ketamine (1.0 mL; 100 mg mL<sup>-1</sup>) and xylazine (0.5 mL; 20 mg mL<sup>-1</sup>). An intraperitoneal injection protocol was followed using a dose of 0.1 mL per 10 g of body weight.

### Cytokine assay

Cytokine levels in mice's serum were measured using the IL-5 ELISA (Fisher Scientific, Fairlawn, NJ, USA). Commercially available kits (Endogen Inc., Cambridge, MA, USA) were used for the IFN- $\gamma$  and IL-4 measurements. The ELISA plates were covered with cytokine-specific detection antibody (Ab; 0.5 mg mL<sup>-1</sup>) overnight at 4 °C. The plates were washed with a phosphate buffer saline (PBS;  $\times 4$ ), Tween-20 (0.05%), and incubated with PBS for 30 min followed by bovine serum albumin (BSA; 2%) at 37 °C. After washing, the supernatant fluids were added to the pits and incubated for 2 h at 37 °C or left overnight at 4 °C, and Ab concentration (0.5 mg mL<sup>-1</sup>) was detected. The ELISA plates were developed and amplified using the VECTASTAIN ABC kit (Vector Laboratories, Burlingame, CA, USA) according to the manufacturer's protocol.

### The experimental work and statistical analysis

The current study is a complete randomized design in which each test was performed four times for each parameter. The experimental work was carried out at the Central Laboratory at Al-Nahrain University and the Materials Research Department, Ministry of Science and Technology, Iraq. The current study was conducted between September 2018 and January 2019. Ethical approval has been obtained before the start of the work. The average was expressed mean  $\pm$  standard deviation, and the significance of the difference was tested for  $P < 0.05$ . The SPSS® statistical package, version 22.0 (SPSS Inc., Chicago, IL, USA) for Windows®, was used.

## Results

### Biosynthesis of AgNPs with *A. terreus*

Initially, the biosynthesis of AgNPs using *A. terreus* was induced. *A. terreus* was cultured on Czapek Dox Agar (Sigma-Aldrich, St. Louis, MO, USA) at 25 °C for a week<sup>29</sup>. Silver nitrate was incubated with *A. terreus* in a controlled environment. Initially, the surface of the fungal colonies was light yellow. After the addition of AgNO<sub>3</sub> solution, the color shifts from transparent yellow to brown confirming the reduction of cationic silver into metallic silver; this indicates the successful production of AgNPs (Figures 1 and 2). Also, the formation of AgNPs was confirmed by ultraviolet-visible (UV-VIS) spectroscopy (JASCO Corp., Tokyo, Japan). The UV-VIS spectrum of AgNPs showed an absorption band at 439 nm as a result of the excitation of surface plasmon vibrations, which is consistent with the literature<sup>30</sup>.

### Atomic force microscopy (AFM)

The particle size of AgNPs synthesized with *A. terreus*

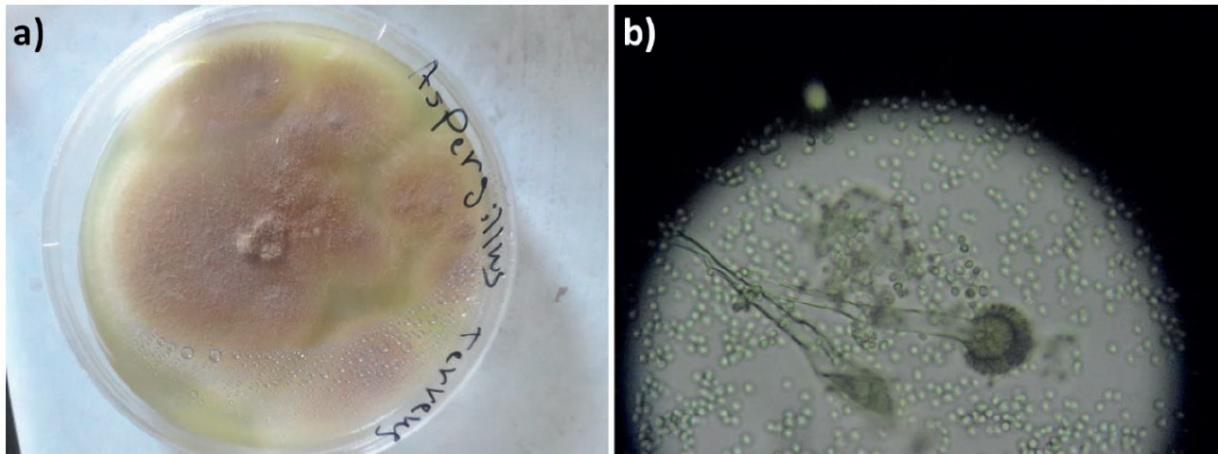


**Figure 1.** *A. terreus* cultured on Czapek Dox Agar at  $25 \pm 2$  °C for a week: a) Colonies in a Petri dish with a diameter of 4 cm; b) Colonies under a light microscope (40 $\times$ ).



**Figure 2.** Synthesis of AgNPs: a) AgNO<sub>3</sub> (1 mM) solution; b) *A. terreus* biomass (50 mL); c) Color alteration of filtrate after incubation in the dark.

was determined using the atomic force microscopy (AFM) (Hitachi High-Technologies, Minato City, Tokyo, Japan). The two- and three-dimensional AFM images (2  $\mu$ m) of the synthesized AgNPs are shown in Figure 3. The AFM images showed the formation of nanoparticles that have a different particle size distribution (20–30 nm) with an average diameter of 25.1 nm. Such AgNPs particle size is appropriate for delivering silver nanoparticles to treat animals' infection with *Candida*<sup>31</sup>. The absorption band appeared at 332 nm in the UV-VIS spectra (Figures S1 and S2) due to the absorption of Ag<sup>+</sup> or other elements in the culture medium.

### Scanning electron microscopy (SEM)

The SEM can determine the external morphology of nanoparticles. Figure 4 shows the SEM images of the AgNPs synthesized with *A. terreus*. The images revealed that the particles displayed a distinctive morphology with a considerable variation in particle size and small numbers of aggregations. Also, they showed the formation of typically visually, small, and uniformly spherical-shape particles of multiple sizes.

### Cytokines assay

The cytokines level: IL-4 and IFN- $\gamma$  were measured four times in the serum of 20 mice, which had been divided into four groups ( $n = 5$  within each group), and the averages were calculated. A blood sample was withdrawn from each mouse to obtain serum for cytokine level analysis after the 21 days trial. Table 1 shows the cytokine serum concentration among four

different groups of mice that have been measured using the enzyme-linked immunosorbent assay (ELISA) plates. The level of cytokines: IL-4 and IFN- $\gamma$  was significantly ( $P < 0.05$ ) higher in the group of mice infected with *C. glabrata* (10<sup>5</sup>, 0.2 mL) compared to those obtained within the control group (natural level). While the cytokines level remains close to the average concentration in mice administrated with AgNPs, such a result was comparable with that obtained in the fourth group of mice (*Candida*-treated *Aspergillus*) after treatment by AgNPs.

The blood of infected mice administered with AgNPs synthesized with *A. terreus* was observed to have an average cytokine level. Such results indicate that AgNPs do not disadvantageously affect the cytokine level. It is worth noting, the level of cytokine returned to its average concentration after treatment, except for the group that has been administrated with *Candida*.

### Discussion

The synthesis of AgNPs with *A. terreus* was confirmed through an alteration in color from transparent yellow to brown after incubation in a dark room. Additionally, AgNPs synthesized with *A. terreus* was confirmed by UV-VIS spectroscopy<sup>30,32</sup>. *A. terreus*, which is unconventional mycobiossystem for synthesizing AgNPs, is cost-effective, highly-stable, and reproducible. Previous research has shown that nanoparticles can significantly inhibit fungi's mechanism of action,

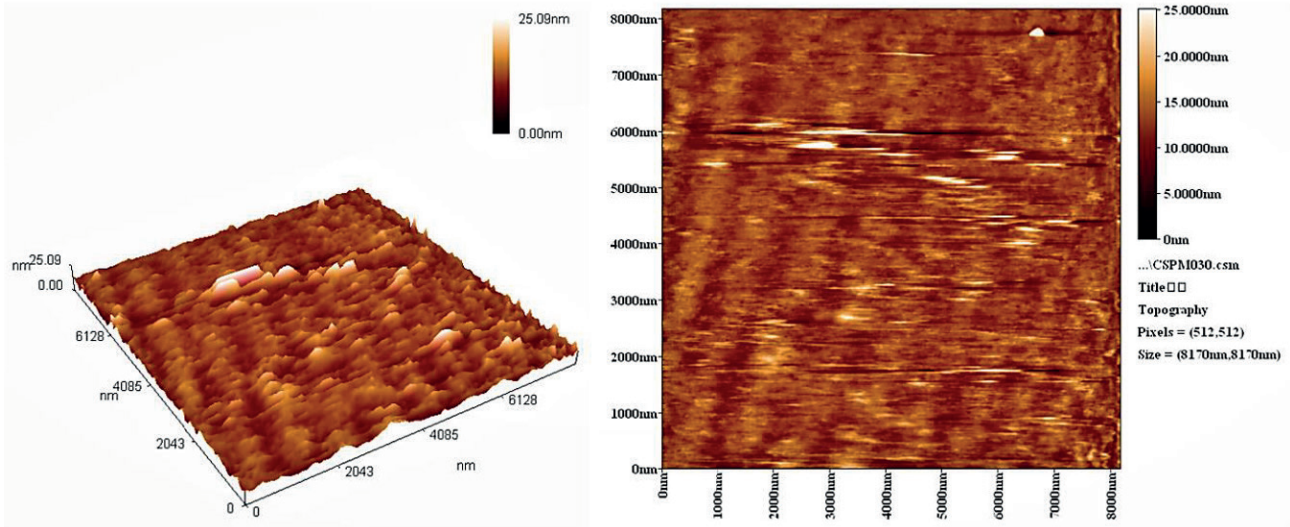


Figure 3. The 2- and 3-dimensional AFM images of AgNPs synthesized with *A. terreus*.

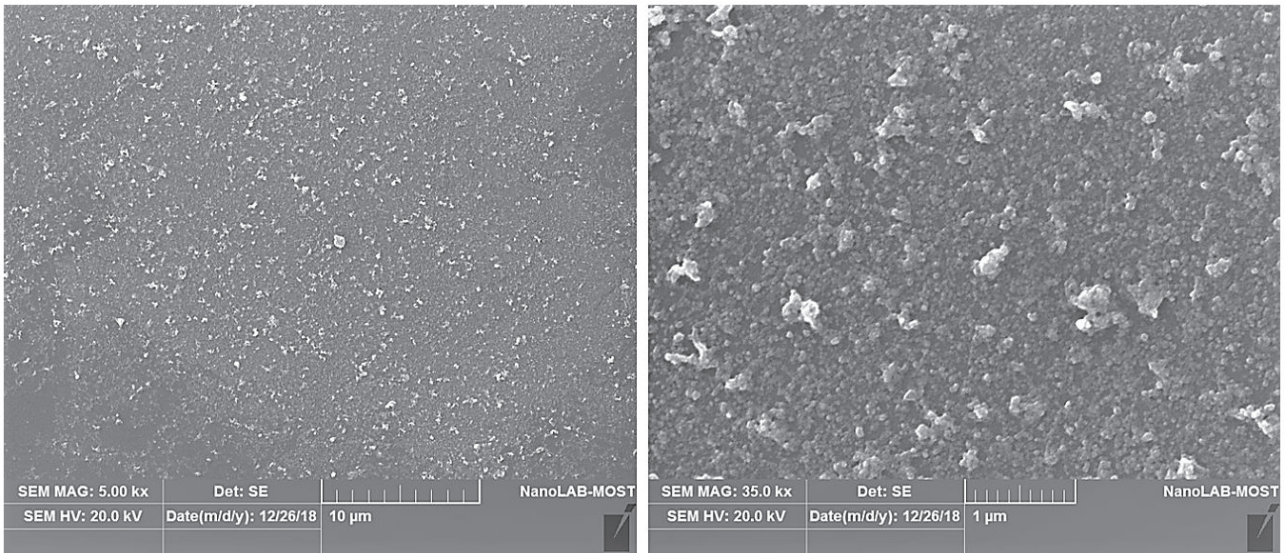


Figure 4. The SEM images for AgNPs synthesized with *A. terreus*.

| Treatment/parameter                      | IL-4        | INF-γ       |
|--|-------------|-------------|
| Control                                  | 0.30 ± 0.01 | 0.38 ± 0.01 |
| <i>Candida</i> *                         | 0.37 ± 0.00 | 0.45 ± 0.00 |
| AgNPs                                    | 0.30 ± 0.01 | 0.37 ± 0.01 |
| <i>Candida</i> treated <i>A. terreus</i> | 0.33 ± 0.01 | 0.40 ± 0.01 |
| LSD $P \leq 0.05$                        | 0.02        | 0.02        |

\* Statistically significant value at  $P < 0.05$ .

Table 1. Cytokine serum levels ( $\text{pg mL}^{-1}$ ) among four different groups of mice.

which provides nanoparticles with unique characteristics in being potent broadband antifungal agents and active drug carriers<sup>33</sup>. The morphological AFM examination of some biologically synthesized AgNPs showed the presence of more than one distinctive particle<sup>34</sup>. The particle size distribution of AgNPs with *A. terreus* showed an average particle size of 25 nm, which is in agreement with the previous research<sup>35</sup>. The particle size of AgNPs biosynthesized using *Pseudomonas aeruginosa* showed multiple particle sizes that ranged from 33 to 300 nm. The majority of particles have a size of 50–100 nm<sup>36</sup>. Small-sized nanoparticles showed better antimicrobial

activity than large-sized nanoparticles due to the particle's large surface area<sup>37</sup>.

At times, no apparent changes were detected using the SEM within the AgNPs, since aggregated tiny particles were produced due to the coating agent<sup>38</sup>. The antimicrobial activity of AgNPs was found to be dependent on the concentration of nanoparticles used<sup>39</sup>. The AgNPs synthesized with *A. terreus* showed vigorous antifungal activity against pathogenic fungi such as *Candida albicans*<sup>24</sup>. Besides, AgNPs showed significant inhibition activity against three types of filamentous fungi that are resistant to antifungal agents such as fluconazole<sup>40</sup>.

The cytokine levels in the serum of mice infected with *Candida spp.* revealed that the immune system response was diverse among different organs. Such an observation could have a critical effect on treatment strategy using immunomodulatory methods<sup>41,42</sup>. It has been established that resistance to candidiasis is related to the progress of the response that is based on IFN- $\gamma$  secretion<sup>43</sup>. A fatal result is associated with the progress of response, which is based on IL-4, IL-13, and IL-10 secretion and IL-5 response<sup>44</sup>. The alteration in colonization patterns of *Candida spp.* in infection-resistant BALB/c mice and infection-prone mice after the infection is associated with the secretion of the cytokines: IFN- $\gamma$ , IL-4, and IL-12<sup>45</sup>. In primary spread candidiasis, IL-4 may hinder *Candida* infection by promoting effector mediators of resistance; for example, IL-4 can promote the growth of a defensive Th1 response in candidiasis<sup>41</sup>. In another study, a detectable level of inspired IL-4 production was present in both the control and infected mice groups. The susceptibility of the infected mice group was higher than that for the control group concerning IL-4 production. Consistent with the current results, a high level of IL-4 was detected in mice infected with candidiasis<sup>46</sup>. Another study revealed that mice with low levels of IL-4 were more susceptible to infection than normal control group<sup>47</sup>.

## Conclusions

Silver nanoparticles using *Aspergillus terreus* were synthesized through a green, simple, fast, and eco-friendly process. This method has the potential to replace the traditional biochemical methods for the production of nanoparticles. The surface morphology of the synthesized nanoparticles was investigated using different techniques and showed an average particle diameter of 25 nm. Silver nanoparticles synthesized with *Aspergillus terreus* were used to investigate the response of cytokines, IL-4 and IFN- $\gamma$  in mice infected with *Candida spp.* The cytokines: IL-4 and IFN- $\gamma$  levels were significantly ( $P < 0.05$ ) higher in mice infected with *C. glabrata* compared to the control group. The mice administered with AgNPs synthesized with *A. terreus* showed an average cytokine level: IL-4 and IFN- $\gamma$ . The cytokines level returned to its normal range after treatment, except for the group that had been administrated with *Candida*.

## Conflicts of Interest

The authors declare no conflict of interest.

## Acknowledgements

The authors are grateful to the Deanship of Scientific Research, King Saud University, for funding through the Vice Deanship of Scientific Research Chairs. We thank Al-Nahrain and Al-Mansour Universities for their technical support.

## Bibliographic references

1. Saikkonen K. Forest structure and fungal endophytes. *Fungal Biol Rev* 2007; 21(1-2): 67-74. doi:10.1016/j.fbr.2007.05.001.
2. Lia M-Y, Hsu J-F, Chu S-M, Wu I-H, Huang H-R, Chiang M-C, Fu R-H, Tsai M-H. Risk factors and outcomes of recurrent Candidemia in children: relapse or re-infection. *J Clin Med* 2019; 8(1): 99. doi:10.3390/jcm8010099.
3. Cleveland AA, Harrison LH, Farley MM, Hollick R, Stein B, Chiller TM, Lockhart SR, Park BJ. Declining incidence of candidemia and the shifting epidemiology of *Candida* resistance in two US metropolitan areas, 2008-2013: results from population-based surveillance. *PLoS One* 2015; 10(3): e0120452. doi:10.1371/journal.pone.0120452.

4. Lai C-C, Wang C-Y, Liu WL, Huang Y-T, Hsueh P-R. Time to positivity of blood cultures of different *Candida* species causing fungemia. *J Med Microbiol* 2012; 61(Pt 5): 701-704. doi:10.1099/jmm.0.038166-0.
5. Giri S, Kindo AJ. A review of *Candida* species causing blood stream infection. *Indian J Med Microbiol* 2012; 30(3): 270-278. doi:10.4103/0255-0857.99484.
6. Pappas PG, Kauffman CA, Andes DR, Clancy CJ, Marr KA, Ostrosky-Zeichner L, Reboli AC, Schuster MG, Vazquez JA, Walsh TJ, Zaoutis TE, Sobel JD. Clinical practice guideline for the Management of Candidiasis: 2016 update by the Infectious Diseases Society of America. *Clin Infect Dis* 2016; 62(4): e1-e50. doi:10.1093/cid/civ933.
7. Colombo AL, Nucci M, Park BJ, Nouér SA, Arthington-Skaggs B, da Matta DA, Warnock D, Morgan J. Epidemiology of candidemia in Brazil: a nationwide sentinel surveillance of candidemia in eleven medical centers. *J Clin Microbiol* 2006; 44(8): 2816-2823. doi:10.1128/JCM.00773-06.
8. Lee W-J, Hsu J-F, Lai M-Y, Chiang M-C, Lin H-C, Huang H-R, Wu I-H, Chu S-M, Fu R-H, Tsai M-H. Factors and outcomes associated with candidemia caused by non-albicans *Candida spp.* versus *Candida albicans* in children. *Am J Infect Control* 2018; 46(12): 1387-1393. doi:10.1016/j.ajic.2018.05.015.
9. Han X, Xu K, Taratula O, Farsad K. Applications of nanoparticles in biomedical imaging. *Nanoscale* 2019; 11(3): 799-819. doi:10.1039/C8NR07769J.
10. Khan I, Saeed K, Khan I. Nanoparticles: properties, applications and toxicities. *Arab J Chem* 2019; 12(7): 908-931. doi:10.1016/j.arabjc.2017.05.011.
11. Alsaba MT, Al Dushaishi MF, Abbas AK. A comprehensive review of nanoparticles applications in the oil and gas industry. *J Petrol Explor Prod Technol* 2020; 10: 1389-1399. doi:10.1007/s13202-019-00825-z.
12. Dahoumane SA, Jeffryes C, Mechouet M, Agathos SN. Biosynthesis of inorganic nanoparticles: a fresh look at the control of shape, size and composition. *Bioengineering* 2017; 4(1): 14. doi:10.3390/bioengineering4010014.
13. Rahman A, Lin J, Jaramillo FE, Bazylinski DA, Jeffryes C, Dahoumane SA. In vivo biosynthesis of inorganic nanomaterials using eukaryotes—A review. *Molecules* 2020; 25(14): 3246. doi:10.3390/molecules25143246.
14. Menon S, Shanmugam R, Kumar VS. A review on biogenic synthesis of gold nanoparticles, characterization, and its applications. *Resource-Efficient Technol* 2017; 3(4): 516-527. doi:10.1016/j.refit.2017.08.002.
15. Guzmán MG, Jean Dille J, Godet S. Synthesis of silver nanoparticles by chemical reduction method and their antibacterial activity. *J Exp Nanosci* 2016; 11(9): 714-721. doi:10.1080/17458080.2016.1139196.
16. Gurunathan S, Park JH, Han JW, Kim JH. Comparative assessment of the apoptotic potential of silver nanoparticles synthesized by *Bacillus tequilensis* and *Calocybe indica* in MDA-MB-231 human breast cancer cells: Targeting p53 for anticancer therapy. *Int J Nanomed* 2015; 10(1): 4203-4222. doi:10.2147/IJN.S83953.
17. Guilger-Casagrande M, de Lima R. Synthesis of silver nanoparticles mediated by fungi: a review. *Front Bioeng Biotechnol* 2019; 7: 287. doi:10.3389/fbioe.2019.00287.
18. Li G, He D, Qian Y, Guan B, Gao S, Cui Y, Yokoyama K, Wang L. Fungus-mediated green synthesis of silver nanoparticles using *Aspergillus terreus*. *Int J Mol Sci* 2012; 13(1): 466-476. doi:10.3390/ijms13010466.
19. Abd El-Aziz ARM, Al-Othman MR, Eifan SA, Mahmoud MA, Marjashi M. Green synthesis of silver nanoparticles using *Aspergillus terreus* (KC462061). *Dig J Nanomater Bios* 2013; 8(3): 1215-1225.
20. Verma VC, Kharwar RN, Gange AC. Biosynthesis of antimicrobial silver nanoparticles by the endophytic fungus *Aspergillus clavatus*. *Nanomedicine (Lond)* 2010; 5(1): 33-40. doi:10.2217/nnm.09.77.

21. Costa Silva LP, Oliveira JP, Keijok WJ, Silva AR, Aguiar AR, Guimarães MCC, Ferraz CM, Araújo JV, Tobias FL, Braga FR. Extracellular biosynthesis of silver nanoparticles using the cell-free filtrate of nematophagus fungus *Duddingtonia flagans*. *Int J Nanomedicine* 2017; 12: 6373–6381. doi:10.2147/IJN.S137703.
22. Shahzad A, Saeed H, Iqtedar M, Hussain SZ, Naz S, Saleem F, Aihetasham A, Chaudhary A. Size-controlled production of silver nanoparticles by *Aspergillus fumigatus* B7CB10: likely antibacterial and cytotoxic effects. *J Nanomater* 2019; 2019: 5168698. doi:10.1155/2019/5168698.
23. Rani R, Sharma D, Chaturvedi M, J P Yadav. Green synthesis, characterization and antibacterial activity of silver nanoparticles of endophytic fungi *Aspergillus terreus*. *J Nanomed Nanotechnol* 2017; 8(4): 1000457. doi:10.4172/2157-7439.1000457.
24. Li G, He D, Qian Y, Guan B, Gao S, Cui Y, Yokoyama K, Wang L. Fungus-mediated green synthesis of silver nanoparticles using *Aspergillus terreus*. *Int J Mol Sci* 2012; 13(1): 466–476. doi:10.3390/ijms13010466.
25. Hossain MM, Polash SA, Takikawa M, Shubhra RD, Saha T, Islam Z, Hossain S, Hasan MA, Takeoka S, Sarker SR. Investigation of the antibacterial activity and *in vivo* cytotoxicity of biogenic silver nanoparticles as potent. *Front. Bioeng. Biotechnol* 2019; 7: 239. doi:10.3389/fbioe.2019.00239.
26. Ray S, Sarkar S, Kundu S. Extracellular biosynthesis of silver nanoparticles using the mycorrhizal mushroom *Tricholoma crassum* (Berk.) Sacc: its antimicrobial activity against pathogenic bacteria and fungus, including multidrug resistant plant and human bacteria. *Dig J Nanomater Bios* 2011; 6(3): 1289–1299.
27. Romani L. Immunity to fungal infections. *Nat Rev Immunol* 2004; 11(4): 275–288. doi:10.1038/nri2939.
28. Romani L, Mencacci A, Grohmann U, Mocci S, Mosci P, Puccetti P, Bistoni F. Neutralizing antibody to interleukin 4 induces systemic protection and T helper type 1-associated immunity in murine candidiasis. *J Exp Med* 1992; 176(1): 19–25. doi:10.1084/jem.176.1.19.
29. Arabatzis M, Velegraki A. Sexual reproduction in the opportunistic human pathogen *Aspergillus terreus*. *Mycologia* 2013; 105(1): 71–79. doi:10.3852/11-426.
30. Botcha S, Prattipati SD. Green synthesis of silver nanoparticles using *Hyptis suaveolens* (L.) Poit leaf extracts, their characterization and cytotoxicity evaluation against PC-3 and MDA-MB 231 cells. *Biologia* 2019; 74(7): 783–793. doi:10.2478/s11756-019-00222-1.
31. Abd El-Aziz ARM, Al-Othman MR, Al-Sohaibani SA, Mahmoud MA, Sayed SRM. Extracellular biosynthesis and characterization of silver nanoparticles using *Aspergillus niger* isolated from Saudi Arabia (strain ksu-12). *Dig J Nanomater Bios* 2012; 7(4): 1491–1499.
32. Ammar HAM, El-Desouky TA. Green synthesis of nanosilver particles by *Aspergillus terreus* HAIN and *Penicillium expansum* HA2N and its antifungal activity against mycotoxigenic fungi. *J Appl Microbiol* 2016; 121(1): 89–100. doi:10.1111/jam.13140.
33. Wang L, Hu C, Shao L. The antimicrobial activity of nanoparticles: present situation and prospects for the future. *Int J Nanomedicine* 2017; 12: 1227–1249. doi:10.2147/IJN.S121956.
34. Ishida K, Cipriano TF, Rocha GM, Weissmüller G, Gomes F, Miranda K, Rozental S. Silver nanoparticle production by the fungus *Fusarium oxysporum*: nanoparticle characterization and analysis of antifungal activity against pathogenic yeasts. *Mem Inst Oswaldo Cruz* 2014; 109(2): 220–228. doi:10.1590/0074-0276130269.
35. Lai C-C, Wang C-Y, Liu W-L, Huang Y-T, Liao C-H, Hsueh P-R. Time to positivity in blood cultures of staphylococci: clinical significance in bacteremia. *J Infect* 2011; 62(3): 249–251. doi:10.1016/j.jinf.2011.01.004.
36. Peiris MK, Gunasekara CP, Jayaweera PM, Arachchi NDH, Fernando N. Biosynthesized silver nanoparticles: are they effective antimicrobials? *Mem Inst Oswaldo Cruz* 2017; 112(8): 537–543. doi:10.1590/0074-02760170023.
37. Vanaja M, Annadurai G. *Coleus aromaticus* leaf extract mediated synthesis of silver nanoparticles and its bactericidal activity. *Appl Nanosci* 2013; 3(3): 217–23. doi:10.1007/s13204-012-0121-9.
38. Birla SS, Gaikwad SC, Gade AK, Rai MK. Rapid synthesis of silver nanoparticles from *Fusarium oxysporum* by optimizing physicochemical conditions. *Sci World J* 2013; 2013: 796018. doi:10.1155/2013/796018.
39. Khan SS, Mukherjee A, Chandrasekaran N. Studies on interaction of colloidal silver nanoparticles (SNPs) with five different bacterial species. *Colloids Surf B Biointerfaces* 2011; 87(1): 129–138. doi:10.1016/j.colsurfb.2011.05.012.
40. Espinel-Ingroff A, Chaturvedi V, Fothergill A, Rinaldi MG. Optimal testing conditions for determining MICs and minimum fungicidal concentrations of new and established antifungal agents for uncommon molds: NCCLS collaborative study. *J Clin Microbiol* 2002; 40(10): 3776–3781. doi:10.1128/jcm.40.10.3776-3781.2002.
41. Chin VK, Foong KJ, Maha A, Rusliza B, Norhafizah M, Chong PP. Multi-step pathogenesis and induction of local immune response by systemic *Candida albicans* infection in an intravenous challenge mouse model. *Int J Mol Sci* 2014; 15(8): 14848–14867. doi:10.3390/ijms150814848.
42. Thompson A, Griffiths JS, Walke L, da Fonseca DM, Lee KK, Taylor PR, Gow NAR, Orr SJ. Dependence on dectin-1 varies with multiple *Candida* species. *Front Microbiol* 2019; 10: 1800. doi:10.3389/fmicb.2019.01800.
43. Ashman RB, Papadimitriou JM. Production and function of cytokines in natural and acquired immunity to *Candida albicans* infection. *Microbiol Rev* 1995; 59(4): 646–672.
44. Spellberg B, Ibrahim AS, Edwards JE Jr, Filler SG. Mice with disseminated candidiasis die of progressive sepsis. *J Infect Dis* 2005; 192(2): 336–343. doi:10.1086/430952.
45. Blobe GC, Schiemann WP, Lodish HF. Role of transforming growth factor beta in human disease. *N Engl J Med* 2000; 342(18): 1350–1358. doi:10.1056/NEJM200005043421807.
46. Káposzta R, Tree P, Maródi L, Gordon S. Characteristics of invasive candidiasis in gamma interferon and interleukin-4-deficient mice: role of macrophages in host defense against *Candida albicans*. *Infect Immun* 1998; 66(4): 1708–1717.
47. Laura LT, Roberta T, Roberta S, Elio S. Interleukin-4 and -10 exacerbate candidiasis in mice. *Eur J Immunol* 1995; 25: 1559–1565.

**Received:** 14 August 2020

**Accepted:** 25 September 2020